Electronic Supplementary Information (ESI) for Energy & Environmental Science.

Highly doped and exposed Cu(I)-N active sites within graphene towards efficient oxygen reduction for zinc-air battery

Haihua Wu,[ab‡] Haobo Li,[ab‡] Xingfei Zhao,[ab] Qingfei Liu,[ab] Jing Wang,[a] Jianping Xiao,[a] Songhai Xie,[c] Rui Si,[d] Fan Yang,[a] Shu Miao,[a] Xiaoguang Guo,[a] Guoxiong Wang*[a] and Xinhe Bao*[a]

[a]State Key Laboratory of Catalysis, CAS Center for Excellence in Nanoscience, Dalian National Laboratory for Clean Energy, Dalian Institute of Chemical Physics, Chinese Academy of Sciences, Dalian, 116023, China

[b]University of Chinese Academy of Sciences, Beijing, 100039, China

[c]Shanghai Key Laboratory of Molecular Catalysis and Innovative Materials, Department of Chemistry, Fudan University, Shanghai 200433, China

[d]Shanghai Synchrotron Radiation Facility, Shanghai Institute of Applied Physics, Chinese Academy of Sciences, Shanghai 201204, China

[‡]These authors have contributed equally.
*Email: wanggx@dicp.ac.cn; xhbao@dicp.ac.cn

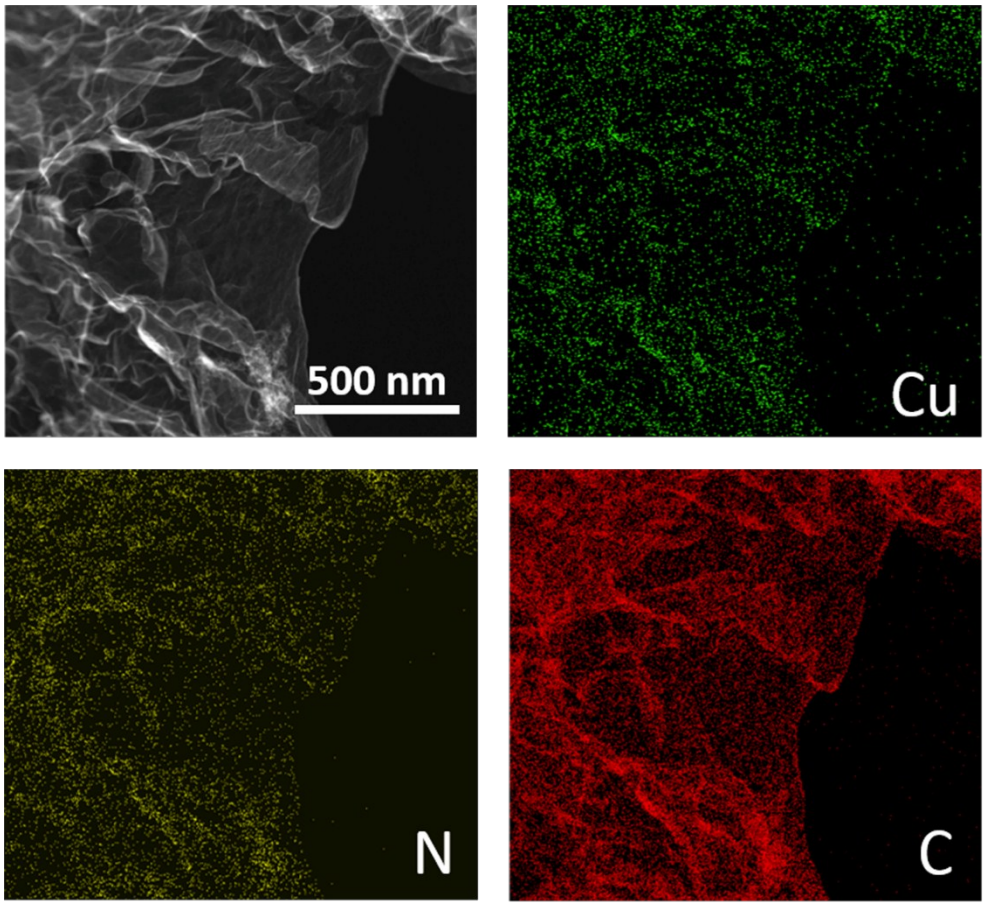

Fig. S1 **Low-resolution** HAADF-STEM image of Cu-N©C-60 and the corresponding element mappings for Cu, N and C atoms.

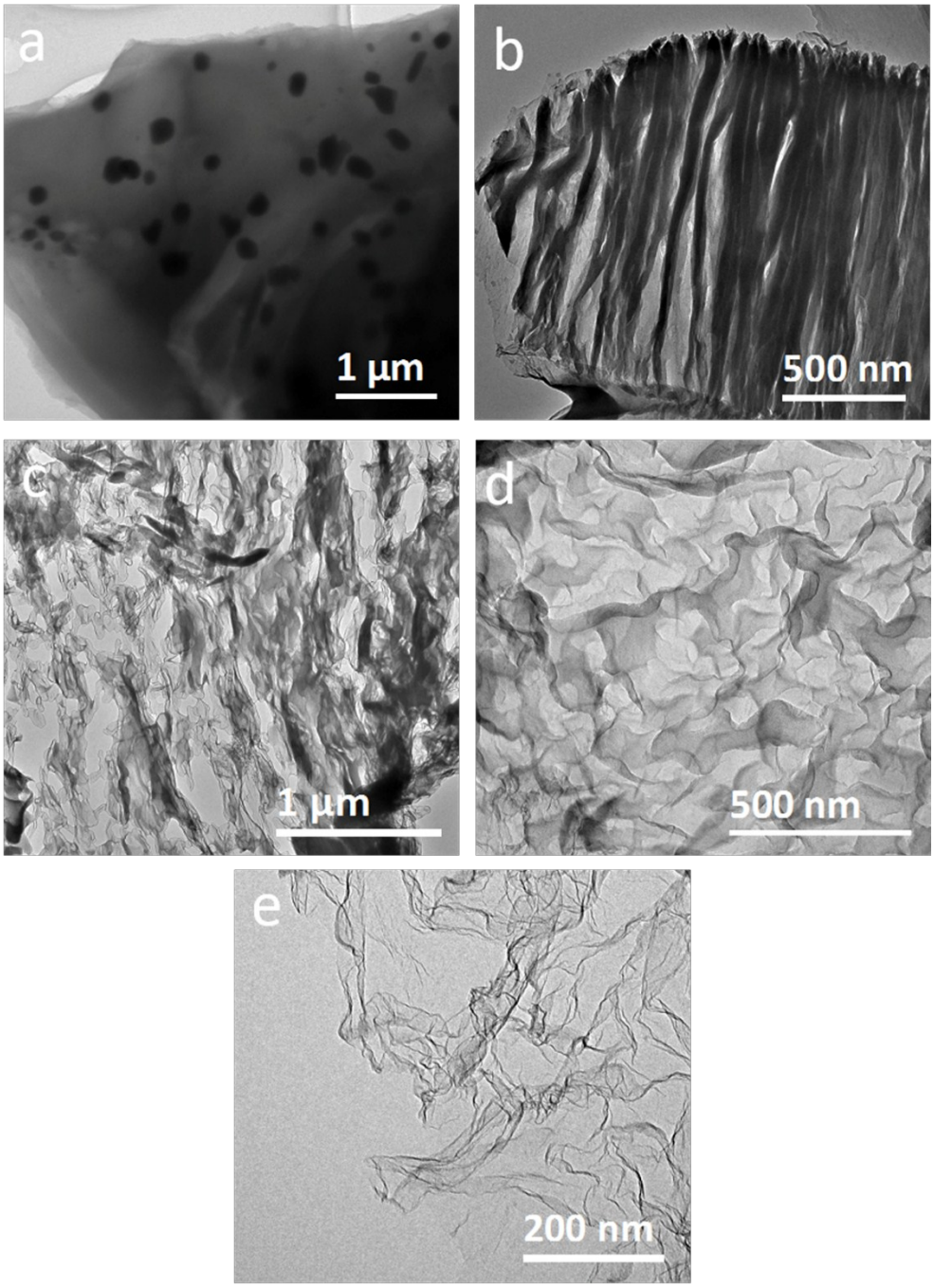

Fig. S2 TEM images of (a) Cu-N©C-0, (b) Cu-N©C-5, (c) Cu-N©C-15, (d) Cu-N©C-30 and (e) Cu-N©C-120.

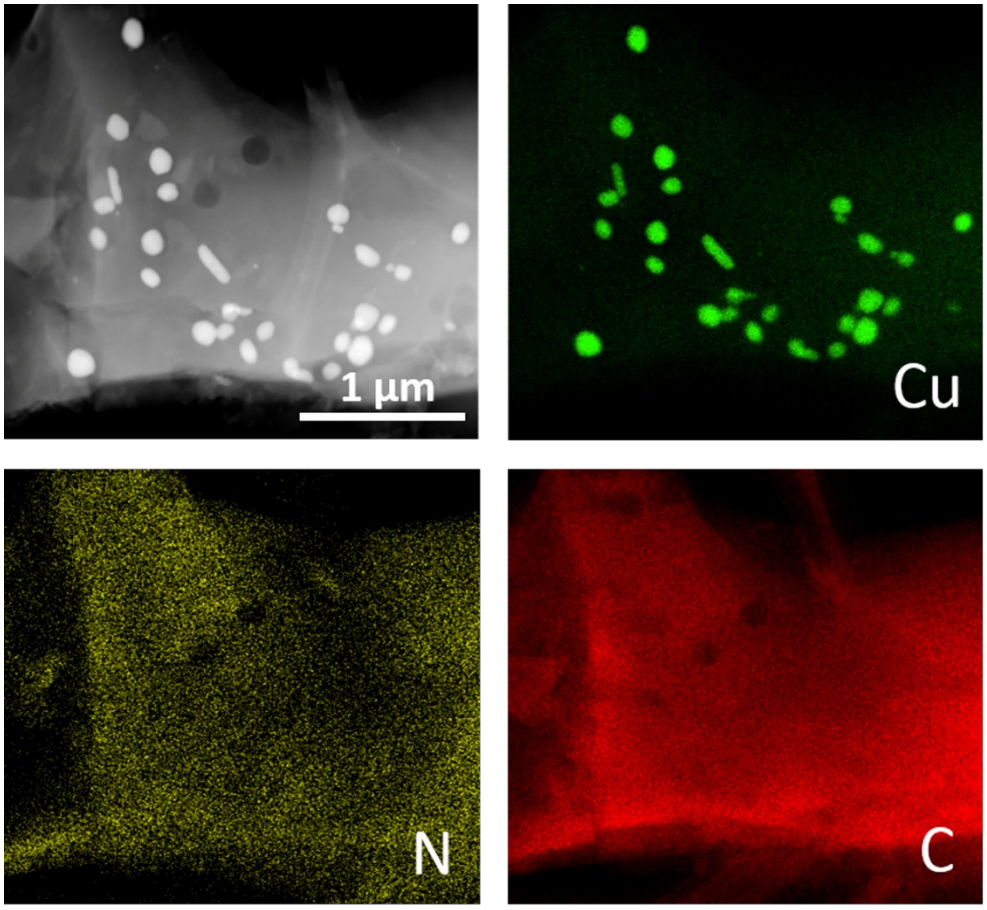

Fig. S3 **Low-resolution** HAADF-STEM image of Cu-N©C-0 and the corresponding element mappings for Cu, N and C atoms.

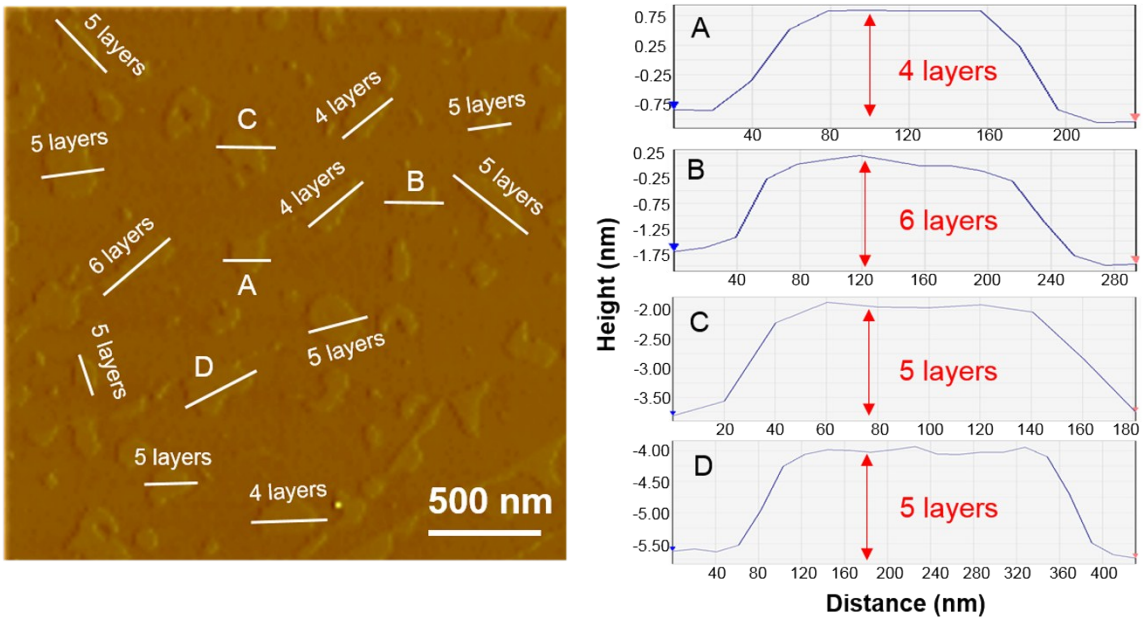

Fig. S4 AFM image of Cu-N©C-60 deposited on an HOPG substrate and the corresponding calculated carbon layers according to theoretical monolayer graphene thickness of 0.34 nm. But the actual layers of samples are probably less because of wrinkle caused by thermal fluctuation.

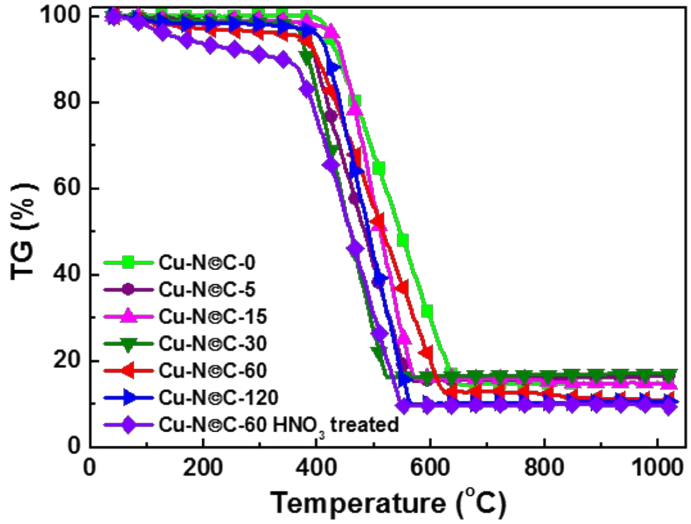

Fig. S5 TG analysis of different samples in air atmosphere.

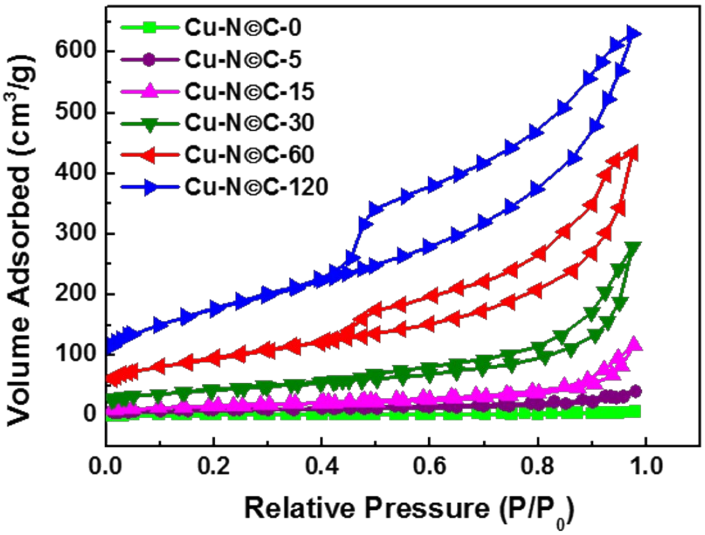

Fig. S6 Nitrogen adsorption–desorption isotherm of different samples.

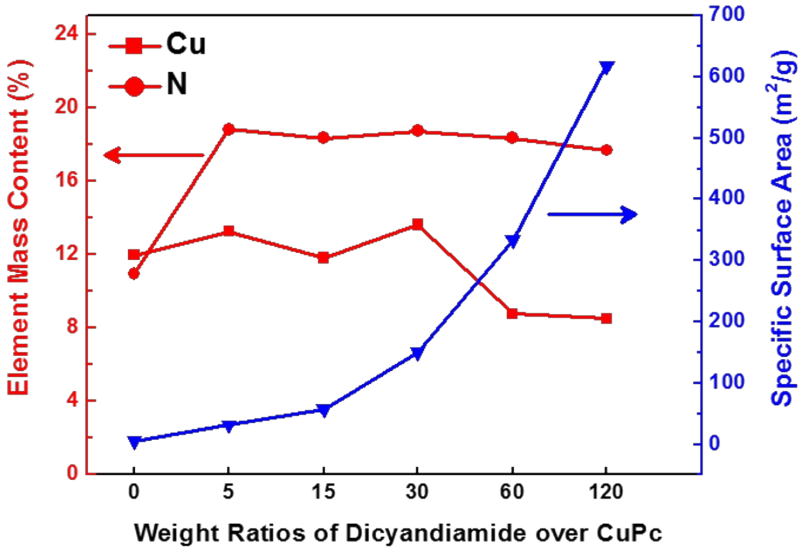

Fig. S7 Element mass contents of Cu, N and specific surface areas of Cu-N©C catalysts.

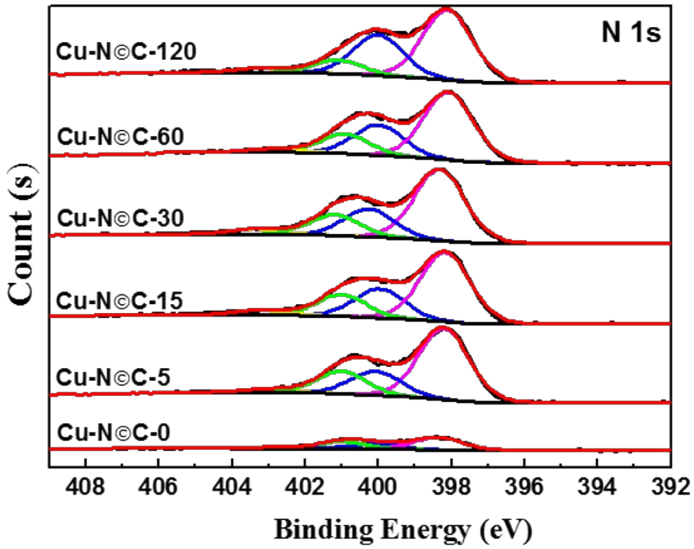

Fig. S8 High-resolution XPS surveys of N 1s for Cu-N©C catalysts.

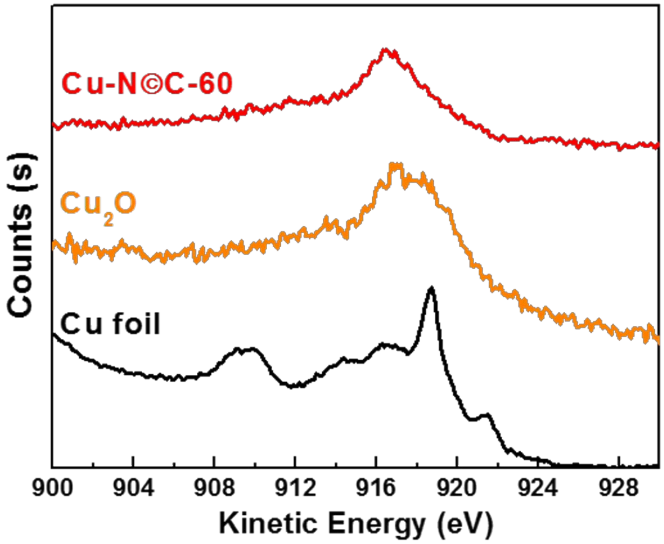

Fig. S9 Cu AES surveys of Cu-N©C-60, Cu_2O and Cu foil.

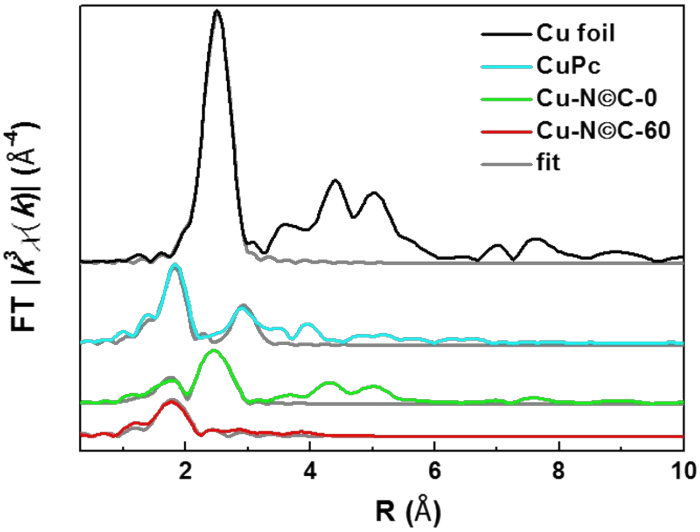

Fig. S10 The Fourier transformed EXAFS spectra and their best fit of different samples. The spectra are phase corrected.

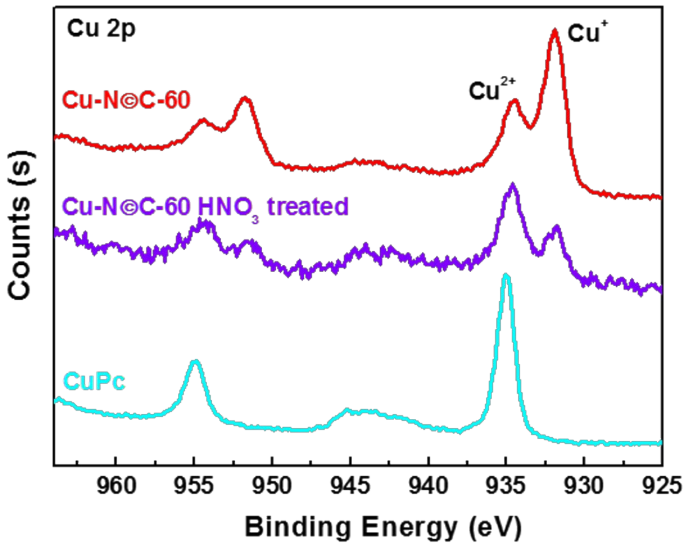

Fig. S11 High-resolution XPS surveys of Cu 2p acquired on Cu-N©C-60 before and after treated by HNO_3 as well as CuPc.

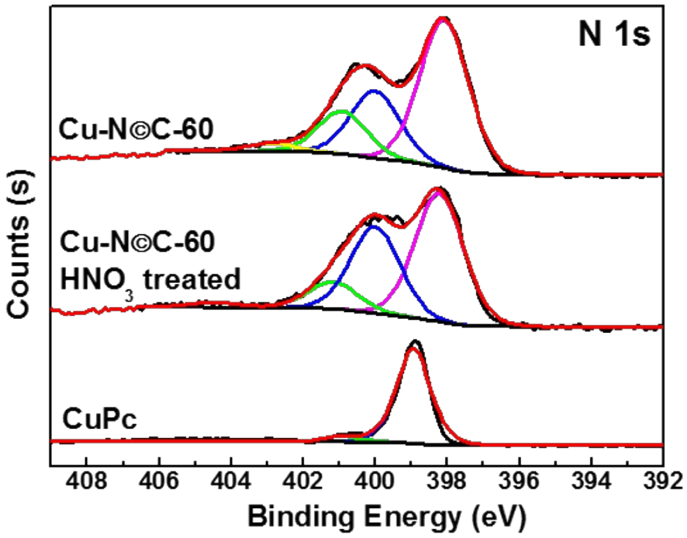

Fig. S12 High-resolution XPS surveys of N 1s acquired on Cu-N©C-60 before and after HNO_3 treatment as well as CuPc.

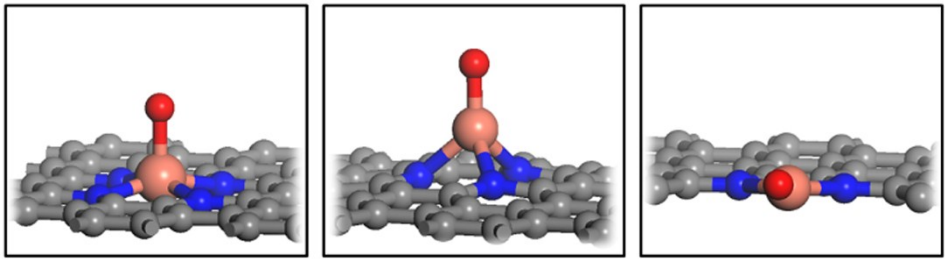

Fig. S13 Optimized atomic structure of one O atom absorbed on Cu-N_4 (left), Cu-N_3 (middle) and Cu-N_2 (right) structures, respectively. The gray, blue, orange, red balls represent C, N, Cu, O atoms, respectively. For Cu-N_3 structure, the Cu atom is stretched out of the graphene plane with O atom binding, thus the structure is instable after O atom adsorption.

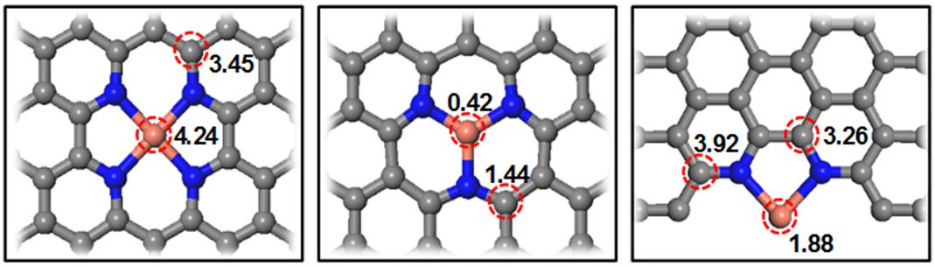

Fig. S14 Calculated adsorption energy of O atoms (ΔE_O) on C and Cu atoms of Cu-N_4 (left), Cu-N_3 (middle) and Cu-N_2 (right) structures, respectively (in units of eV). The gray, blue, orange, red balls represent C, N, Cu, O atoms, respectively. The ΔE_O is defined by: $\Delta E_O = E_{surface+O} - E_{surface} - \mu_O$, where $E_{surface+O}$ is the total energy for the surface with one adsorbed O atom, $E_{surface}$ is the total energy for the catalyst surface, and μ_O is the chemical potential of O with reference to a water molecule: $\mu_O = \mu(H_2O) - \mu(H_2)$. It can be seen that for Cu-N_4, O atoms tend to absorb on C atoms, while for Cu-N_3 and Cu-N_2, O atoms prefer to absorb on Cu atoms.

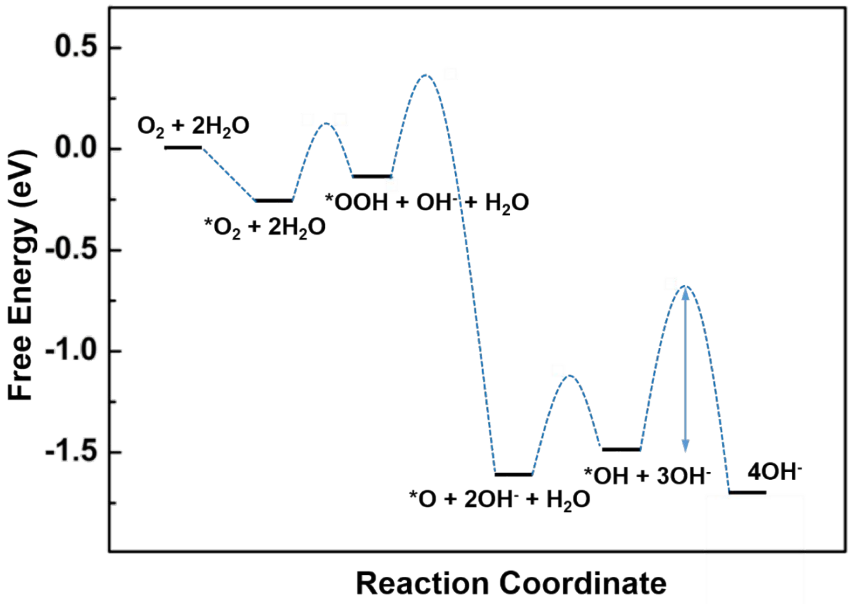

Fig. S15 Free energy diagram for ORR process on Cu-N_2 structure. The rate-determining step is shown in blue arrow, of which the reaction barrier is 0.83 eV for *OH desorption.

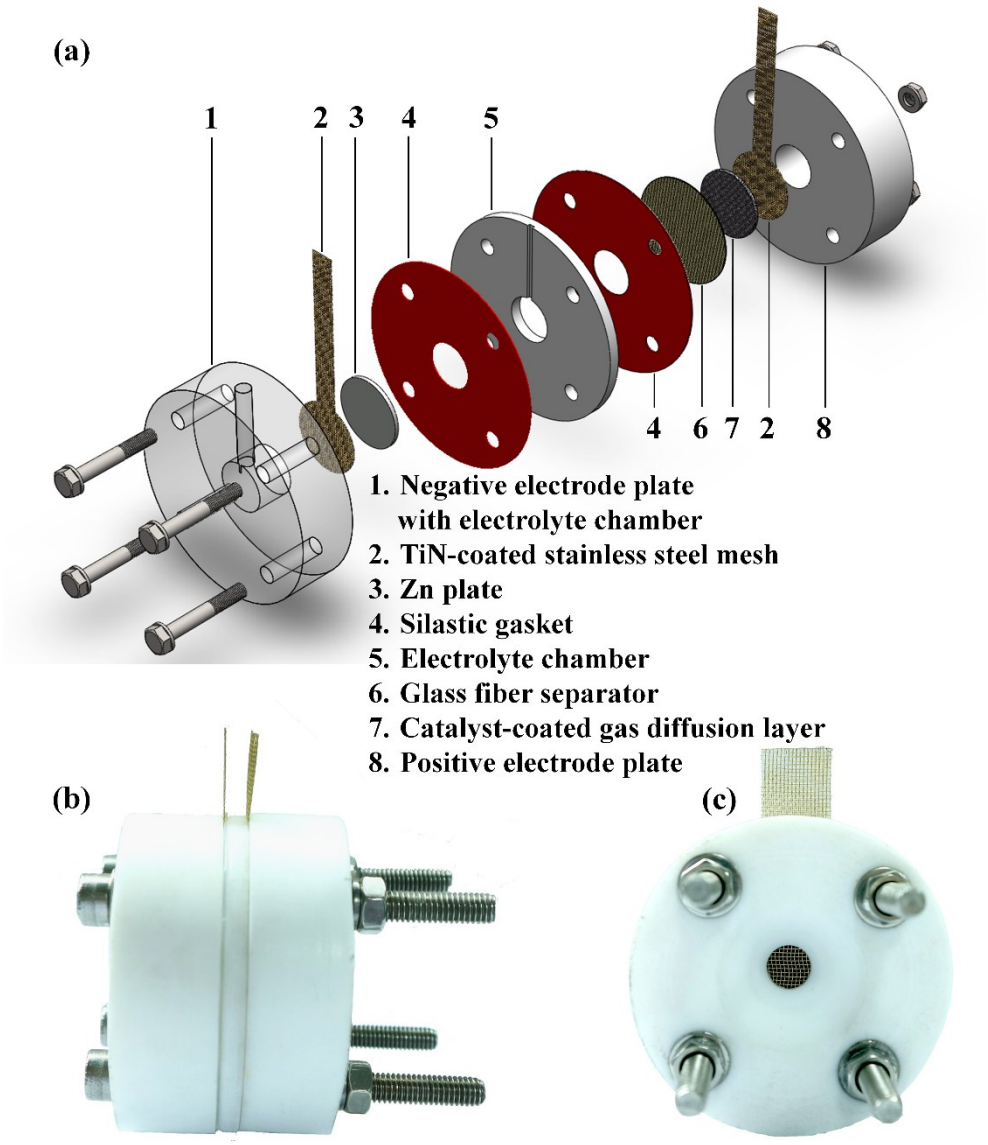

Fig. S16 (a) The schematic diagram and (b), (c) photograph of homemade zinc-air battery.

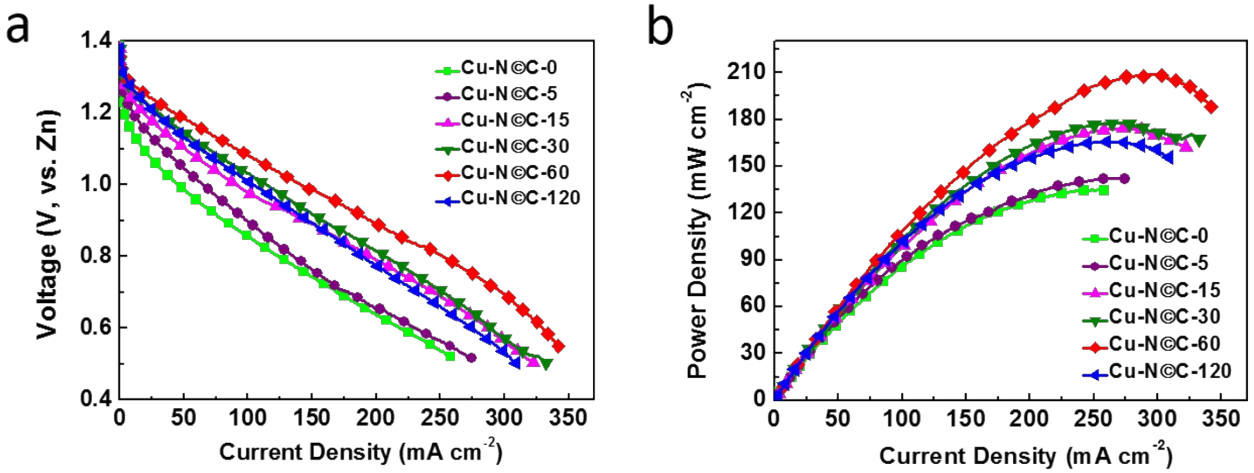

Fig. S17 (a) Discharge curves and (b) the corresponding power density curves of zinc-air batteries with Cu-N©C catalysts. The catalyst loading on the air electrode was 0.4 mg cm^{-2}.

Table S1. Content of Cu in different catalysts.

Catalyst	Cu wt%
Cu-N©C-0	11.98
Cu-N©C-5	13.25
Cu-N©C-15	11.81
Cu-N©C-30	13.62
Cu-N©C-60	8.75
Cu-N©C-120	8.50
Cu-N©C-60 HNO_3 treated	7.44

Table S2. The total nitrogen content and percentage of different nitrogen species in each catalyst.

Catalyst	Total N content (wt%)	Percentage of different N species (wt%)			
		Pyridinic	Pyrrolic	Graphitic	Oxidized
Cu-N©C-0	10.96	5.82	4.49	-	0.64
Cu-N©C-5	18.82	11.04	3.77	3.46	0.41
Cu-N©C-15	18.34	10.12	4.26	3.18	0.78
Cu-N©C-30	18.73	10.61	4.19	3.11	0.83
Cu-N©C-60	18.36	10.23	4.64	2.95	0.53
Cu-N©C-120	17.68	9.59	5.58	1.87	0.65
Cu-N©C-60 HNO_3 treated	17.68	9.20	6.18	1.95	0.35

Table S3. Specific surface area (SSA) of different catalysts.

Catalyst	SSA (m^2/g)
Cu-N©C-0	5.721
Cu-N©C-5	31.846
Cu-N©C-15	57.464
Cu-N©C-30	150.321
Cu-N©C-60	333.877
Cu-N©C-120	618.817

Table S4. EXAFS fitting data.

Sample	Cu-N		Cu-Cu		D. W.	ΔE_0 (eV)
	R (Å)	CN	R (Å)	CNr		
Cu foil	—	—	2.542±0.004	12	0.0087±0.0006	4.2±0.8
Cu-N©C-0	1.90±0.03	1.3±0.3	2.54±0.02	3.0±0.8	0.009±0.002(Cu) 0.003±0.001(O)	4.1±3.6
Cu-N©C-60	1.93±0.03	2.2±0.4	—	—		8.1±5.0
CuPc	1.94±0.01	3.8±0.5	—	—		10.4±1.8

CN is coordination number.

Table S5. Comparison of peak power density (per mass of catalyst) of different primary Zinc-air batteries reported in literatures.

Catalyst	Catalyst loading ($mg\ cm^{-2}$)	Peak power density ($W\ g_{cat}^{-1}$)	Reference
Cu-N©C-60	0.4	525	This work
Fe@N-C-700	2.2	100	1
CoO/N-CNT	1.0	265	2
MnO_2/Co_3O_4	2.0	16.5	3
Co-doped TiO_2	2.0	68	4
CuPt-NC	2.0	125	5
$Co(II)_{1-x}Co(0)_{x/3}Mn(III)_{2x/3}S$	1.0	250	6
Co_3O_4–SP/NGr	1.0	190	7
Nanoporous carbon fiber films	2.0	92.5	8

References

1 J. Wang, H. H. Wu, D. F. Gao, S. Miao, G. X. Wang and X. H. Bao, *Nano Energy*, 2015, **13**, 387-396.

2 Y. G. Li, M. Gong, Y. Y. Liang, J. Feng, J. E. Kim, H. L. Wang, G. S. Hong, B. Zhang and H. J. Dai, *Nat. Commun.*, 2013, **4**, 1805.

3 G. J. Du, X. G. Liu, Y. Zong, T. S. A. Hor, A. S. Yu and Z. L. Liu, *Nanoscale*, 2013, **5**, 4657-4661.

4 L. N. Han, L. B. Lv, Q. C. Zhu, X. Wei, X. H. Li and J. S. Chen, *J. Mater. Chem. A*, 2016, **4**, 7841-7847.

5 V. M. Dhavale and S. Kurungot, *ACS Catal.*, 2015, **5**, 1445-1452.

6 Z. L. Wang, S. Xiao, Y. M. An, X. Long, X. L. Zheng, X. H. Lu, Y. X. Tong and S. H. Yang, *ACS Appl. Mater. Interfaces*, 2016, **8**, 13348–13359.

7 S. K. Singh, V. M. Dhavale and S. Kurungot, *ACS Appl. Mater. Interfaces*, 2015, **7**, 21138-21149.

8 Q. Liu, Y. B. Wang, L. M. Dai and J. N. Yao, *Adv. Mater.*, 2016, **28**, 3000-3006.